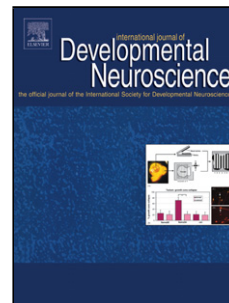


Accepted Manuscript

Title: Characterisation of neuronal and glial populations of the visual system during zebrafish lifespan

Authors: FJ Arenzana, A Santos-Ledo, A Porteros, J Aijón, A Velasco, JM Lara, R Arévalo



PII: S0736-5748(11)00023-2
DOI: doi:10.1016/j.ijdevneu.2011.02.008
Reference: DN 1449

To appear in: *Int. J. Devl Neuroscience*

Received date: 30-11-2010
Revised date: 7-2-2011
Accepted date: 23-2-2011

Please cite this article as: Arenzana, F.J., Santos-Ledo, A., Porteros, A., Aijón, J., Velasco, A., Lara, J.M., Arévalo, R., Characterisation of neuronal and glial populations of the visual system during zebrafish lifespan, *International Journal of Developmental Neuroscience* (2010), doi:10.1016/j.ijdevneu.2011.02.008

This is a PDF file of an unedited manuscript that has been accepted for publication. As a service to our customers we are providing this early version of the manuscript. The manuscript will undergo copyediting, typesetting, and review of the resulting proof before it is published in its final form. Please note that during the production process errors may be discovered which could affect the content, and all legal disclaimers that apply to the journal pertain.

Research Highlights

We analyse the distribution of zn-1, CR and GFAP during zebrafish lifespan

Postmitotic cells of the retina are immunopositive to Zn-1 and calretinin

Optic nerve transiently expresses GFAP when it arrives at the optic tectum

CR is expressed in different cellular types and neuropile in the visual system

Accepted Manuscript

1
2
3
4 **Title page**

5
6 Characterisation of neuronal and glial populations of the visual system during zebrafish
7
8 lifespan.
9

10 *#Arenzana FJ, *Santos-Ledo A, Porteros A, Aijón J, Velasco A, Lara JM and Arévalo R
11
12
13
14

15 * These authors contributed equally to this work
16
17
18
19

20 Dpto. de Biología Celular y Patología. Universidad de Salamanca. Instituto de Neurociencias
21
22 de Castilla y León. Salamanca, E 37007 (Spain)
23
24

25 # Grupo de Neurobiología del Desarrollo-GNDe, Hospital Nacional de Parapléjicos, Finca
26
27 La Peraleda s/n Toledo, E-45071, Spain.
28
29
30
31

32 Number of pages: 30
33
34

35 Number of figures: 5
36
37
38
39
40
41

42 **Corresponding author:**
43

44 Dr. Rosario Arévalo
45

46 Departamento de Biología Celular y Patología.
47

48 Universidad de Salamanca.
49

50 Instituto de Neurociencias de Castilla y León.
51

52 C/ Pintor Fernando Gallego 1
53

54 E-37007 Salamanca. Spain
55

56 Phone: + (34) (923) 294500 ext. 5322
57

58 Fax: + (34) (923) 294549
59

60 E-mail: mraa@usal.es
61
62
63
64
65

Abstract

During visual system morphogenesis, several cell populations arise at different time points correlating with the expression of specific molecular markers. We have analysed the distribution pattern of three molecular markers (zn-1, calretinin and glial fibrillary acidic protein) which are involved in the development of zebrafish retina and optic tectum. Zn-1 is a neural antigen expressed in the developing zebrafish central nervous system. Calretinin is the first calcium-binding protein expressed in the central nervous system of vertebrates and it is widely distributed in different neuronal populations of vertebrate retina, being a valuable marker for its early and late development. Glial fibrillary acidic protein (GFAP), which is an astroglial marker, is a useful tool for characterising the glial environment in which the optic axons develop.

We describe the expression profile changes in these three markers throughout the zebrafish lifespan with special attention to ganglion cells and their projections. Zn-1 is expressed in the first postmitotic ganglion cells of the retina. Calretinin is observed in the ganglion and amacrine cells of the retina in neurons of different tectal bands and in axons of retinofugal projections. GFAP is localised in the endfeet of Müller cells and in radial processes of the optic tectum after hatching. A transient expression of GFAP in the optic nerve, coinciding with the arrival of the first calretinin-immunoreactive optic axons, is observed. As axonal growth occurs in these regions of the zebrafish visual pathway (retina and optic tectum) throughout the lifespan, a relationship between GFAP expression and the correct arrangement of the first optic axons may exist.

In conclusion we provide valuable neuroanatomical data about the best characterised sensorial pathway to be used in further studies such as teratology and toxicology.

Key words: Calretinin, Development, GFAP, zn-1

1. Introduction

The zebrafish has become one of the standard vertebrate models for Developmental Biology and human disease studies (reviewed in: Lieschke and Currie, 2007) including neurological pathologies such as fronto-temporal dementia (Paquet *et al.*, 2009), Alzheimer's disease (Newman *et al.*, 2009; Paquet *et al.*, 2009), Huntington's disease (Henshall *et al.*, 2009), Parkinson's disease (Sheng *et al.*, 2010) and visual disorders (Goldsmith and Harris, 2003; Fadool and Dowling, 2008; Sager *et al.*, 2010). Neuroanatomical studies have described different central nervous system (CNS) populations (catecholaminergic: Holzschuh *et al.*, 2001; Arenzana *et al.*, 2006; cholinergic: Clemente *et al.*, 2004; Arenzana *et al.*, 2005; dopaminergic: Filippi *et al.*, 2007; 2010; Kastnerhuber *et al.*, 2010; GABAergic: Candal *et al.*, 2008; Mueller and Guo, 2009; histaminergic: Kaslin and Panula, 2001; nitrenergic: Holmqvist *et al.*, 2004; orexinergic/hypocretinergic: Prober *et al.*, 2006; Faraco *et al.*, 2006; noradrenergic: Filippi *et al.*, 2007; 2010; Kastnerhuber *et al.*, 2010; serotonergic: McLean and Fetcho, 2004) which have allowed the analysis of the structural alterations present in the mutants obtained after genetic screening (Amsterdam and Hopkins, 2006; Sprague *et al.*, 2008) as well as the analysis of their putative alterations after different pharmacological treatments and/or small molecular screens (i.e. drugs of abuse, xenobiotics, pesticides, nanoparticles...). Most of the studies focus on either development or adulthood, but very few describe the distribution pattern of proteins throughout lifespan. These kinds of analysis are necessary for a better knowledge of the dynamic expression of the proteins, as some of them change their location during development. The analysis throughout lifespan would provide valuable information that can be combined with behavioural and teratogenic analysis. Moreover, the zebrafish visual system has become a model for behaviour, teratogenia and gene expression studies (Parnig *et al.*, 2007; review in Renninger *et al.*, 2011).

1
2
3
4 Zebrafish visual system is one of the best characterised sensorial pathways in vertebrates.
5
6 Different experimental approaches, such as anatomical (Burrill and Easter, 1994; Schmitt and
7
8 Dowling, 1994; Liu *et al.*, 1999), genetic (Karlstrom *et al.*, 1996; Trowe *et al.*, 1996; Cerveny
9
10 *et al.*, 2010) and physiological (Easter and Nicola, 1996; Emran *et al.*, 2010), have been used.
11
12 After the evagination of the optic vesicles, some of the most distal cells originate the neural
13
14 retinal layer and the cells that connect the optic vesicle to the forebrain form the optic stalk and
15
16 differentiate as glial cells (review in Wilson and Houart, 2004). Retinal axons leave the retina
17
18 at 36 hpf, although optic growth cones do not reach the optic tectum (OT) until 46 hpf
19
20 (Stuermer, 1988). The optic axons project topographically onto the OT where they form
21
22 several bands of terminals. The mesencephalic OT is a multi-layered encephalic region
23
24 constituted by six layers according to Vanegas *et al.* (1984) and Meek and Nieuwenhuys
25
26 (1998). All these layers are originated during development from two regions called
27
28 periventricular grey zone (PVGZ) and superficial white zone (SWZ) (Sharma, 1975). This
29
30 nomenclature has been used in several works (Miguel-Hidalgo *et al.*, 1991; Arévalo *et al.*,
31
32 1995; Diaz *et al.*, 2002; Arenzana *et al.*, 2006; Clemente *et al.*, 2008).
33
34
35
36
37
38
39

40 Zn-1, calretinin (CR) and glial fibrillary acidic protein (GFAP) are molecular markers
41
42 that allow the characterisation of specific cell populations in the developing visual pathway of
43
44 zebrafish. Zn-1 is a neural antigen from zebrafish embryos whose distribution pattern has been
45
46 used for describing the segmental organisation of zebrafish hindbrain (Hanneman *et al.*, 1988;
47
48 Trevarrow *et al.*, 1990). CR is the first detectable calcium-binding protein during fish CNS
49
50 development (Porteros *et al.*, 1997, 1998; Candal *et al.*, 2008) and its expression is located,
51
52 among other types, in the ganglion cells of the retina (Weruaga *et al.*, 2000). In fish, GFAP has
53
54 been observed in different glial cellular types like ependimocytes or radial glia in both adult
55
56
57
58
59
60
61
62
63
64
65

1
2
3 animals (Cardone and Roots, 1990; Ito *et al.*, 2010) and embryos (Marcus and Easter, 1995;
4
5
6 Bernardos and Raymond, 2006).

7
8 Although these three molecular markers have been previously used to understand the
9
10 development of the zebrafish visual system, the cell populations that express them, their
11
12 involvement in retinal and optic tectum differentiation and their role in the axonal guidance of
13
14 the optic nerve remain unclear. In the present study, we have analysed the distribution pattern
15
16 of zn-1, CR and GFAP in the zebrafish visual pathway throughout the lifespan, providing
17
18 useful neuroanatomical data for the identification of mutants with visual system disorders after
19
20 genetic screening (Li *et al.*, 2010), for studies in teratology and toxicology, and for
21
22 pharmacogenetic screening in zebrafish models of human visual disorders.
23
24
25
26
27
28
29

30 **2. Material and methods**

31 *2.1 Subjects*

32
33 AB strain zebrafish embryos were obtained by natural mating from our laboratory colony
34
35 and maintained according to standard procedures (Westerfield, 1995). Ages of embryos are
36
37 given as hours postfertilization (hpf) or days postfertilization (dpf). Embryos (from fertilization
38
39 to hatching) of 24, 36, 48 and 60 hpf, larvae (from hatching to yolk re-absorption) of 3, 4 and 5
40
41 dpf, juveniles of 10, 15, 21, 30 and 60 dpf, and adults of 90 dpf and 1 year old were analysed.
42
43 The specimens were anaesthetised with 0.03% tricaine methanesulfonate (MS 222, Sigma-
44
45 Aldrich Inc., St. Louis, MO). All procedures were in accordance with the European
46
47 Communities Directives (86/ 609/ EEC; 2003/65/EC) and the current Spanish legislation for
48
49 the use and care of animals in research (RD 1201/2005; BOE 252/34367-91, 2005), and
50
51 conformed to NIH guidelines.
52
53
54
55
56
57
58
59
60
61
62
63
64
65

2.2 Western blot analysis

In order to verify the specificity of the GFAP antibody in zebrafish CNS, we carried out a Western blot analysis of extracts of retina and brain. Both retinas and brains of zebrafish and mouse were dissected and immediately lysed with 50-100 μ l of 25 mM HEPES (pH 7.7), 0.3 M NaCl, 1.5 mM MgCl₂, 0.2 mM EDTA, 0.1% Triton X-100, 20 mM β -glycerophosphate, 0.1 mM sodium orthovanadate supplemented with protease inhibitors (1 mM phenylmethanesulfonyl fluoride, 20 μ g/ml aprotinin, 20 μ g/ml leupeptin; Sigma-Aldrich, Inc.). After 20 min on ice the solubilised proteins were obtained by centrifugation, boiled in Laemmli sample buffer [2% sodium dodecyl sulphate (SDS), 10% glycerol, 140 mM β -mercaptoethanol, 60 mM Tris-HCl (pH 6.8), 0.01% bromophenol blue]. The proteins were measured with a Bio-Rad Protein Assay kit (Bio-Rad Laboratories, Hercules, CA) (Bradford method). Proteins (20-50 μ g) were separated through 7.5-12% SDS-polyacrylamide gels under reducing conditions. Pre-stained protein molecular mass standards (Bio-Rad Laboratories) were also run in the same gel. After electrophoresis, the proteins were transferred to nitrocellulose filters (Boehringer Mannheim, Indianapolis, IN), blocked with 5% (w/v) powdered defatted milk in TBST (50 mM Tris-HCl, pH 8.0, 150 mM NaCl, 0.1% Tween-20) for 90 min at room temperature and incubated overnight at 4°C with primary mouse monoclonal antibody anti-GFAP (1:4000). The biotinylated secondary antibody horse anti-mouse immunoglobulin G (Vectastain, Vector Laboratories, Inc.) was immunodetected using streptavidin-horseradish peroxidase conjugate (Vector Laboratories Inc.) diluted 1:1000 in TBST and signals were revealed using an enhanced chemiluminescence detection (ECL) system (Amersham Bioscience, Aylesbury, UK). Negative controls were performed by omitting the primary antibody or by substituting it with non-immune rabbit IgG.

2.3 Immunohistochemistry

Embryos, larvae, and heads of juveniles and adults were fixed by immersion overnight at 4 °C with paraformaldehyde 4%. Transverse and parasagittal sections (25 µm thick for adults and juveniles; 12 µm for larvae and embryos) were obtained on a cryostat (Leica, Nussloch, Germany) and thaw-mounted on gelatin-coated slides. The immunohistochemical technique was performed as previously described (Clemente *et al.*, 2004, Arenzana *et al.*, 2005; Arenzana *et al.*, 2006). Mouse monoclonal antibody (1:300) against zn-1 (Developmental Studies Hybridoma Bank, Iowa City, IA), rabbit polyclonal antibody (CR 7696; Swant, Bellinzona, Switzerland) (1:10000) against CR, and mouse monoclonal antibody (1:400) against GFAP (Incstar, Stillwater, MN) were employed. The secondary antibodies for anti-zn-1 and anti-GFAP were biotinylated horse anti-mouse immunoglobulin G (Vectastain, Vector Laboratories, Inc., Burlingame, CA) or Cy5-goat anti-mouse immunoglobulin G (Jackson ImmunoResearch Laboratories Inc., West Grove, PA), while for CR immunodetection the secondary antibodies employed were biotinylated goat anti-rabbit immunoglobulin G (Vectastain, Vector Laboratories Inc.) or Cy2-goat anti-rabbit immunoglobulin G (Jackson ImmunoResearch Laboratories Inc.). Nuclei were counterstained with propidium iodide (1:4000).

2.4 Image Analysis

Sections were analysed with a Leica DMLS (Leica Microsystems, Bensheim, Germany) equipped with brightfield condensers. Brightfield digital images were obtained with an Olympus OP-70 digital camera (Olympus Corporation, Tokyo, Japan) coupled to an Olympus Provis AX70 photomicroscope. The capture software was connected to a trichromatic sequential filter (Cambridge Research & Instrumentation Inc., Boston, MA). Fluorescence

1
2
3 images were obtained from a confocal laser scanning microscope (Leica TCS SP2; Leica
4
5
6 Microsystems) coupled to a Leica DM IRE2 (Leica Microsystems) inverted microscope with
7
8 argon- and helium-neon lasers. The original images were processed digitally with Adobe®
9
10 Photoshop® 7.0 (Adobe Systems, San Jose, CA) software. The sharpness, contrast and
11
12 brightness were adjusted to reflect the appearance seen through the microscope.
13
14

17 18 **3. Results**

19
20 In this study, we analysed the neurochemical evolution of the zebrafish retina and OT
21
22 from the embryonic period to adult configuration using the immunohistochemical detection of
23
24 zn-1, CR and GFAP. In order to analyse the relationship between the growing CR-ir optic
25
26 axons and GFAP transient expression in optic nerve at 3 dpf, we carried out a double
27
28 immunolabelling study using confocal microscopy.
29
30

31
32 As a previous step we tested the specificity of GFAP antibody. Western blotting results
33
34 for GFAP showed a single band of 50 kDa in all biological samples, demonstrating the
35
36 specificity of the GFAP antibody in zebrafish CNS (Fig. 1). The specificity of zn-1
37
38 (Developmental Studies Hybridoma Bank) and CR (Castro *et al.*, 2006) had been previously
39
40 reported.
41
42
43

44 45 46 47 *3.1 Zn-1*

48
49 Zn-1 immunoreactivity was observed for the first time in the visual pathway at 36 hpf in
50
51 the retina and the OT. The retina displayed zn-1 immunoreactive (zn-1-ir) pyriform cells
52
53 situated in the central part of the presumptive ganglion cell layer of the retina (GCL) (Fig. 2a),
54
55 while the OT showed zn-1-ir cells located in the periventricular grey zone (PVGZ) (Fig. 2b).
56
57
58 The density of zn-1-ir elements in the zebrafish visual pathway increased at 48 hpf, especially
59
60
61
62
63
64
65

1
2
3 in the retina where staining extended from the central part to the periphery (Fig. 2c). Stained
4
5
6 neuropile in the outer plexiform layer of the retina (OPL) and in the inner plexiform layer of
7
8 the retina (IPL) were observed. Fusiform zn-1-ir cells were situated in the inner nuclear layer
9
10 of the retina (INL) showing stained prolongations at the cellular poles. Cell bodies and axons
11
12 of ganglion cells that constitute the optic nerve were immunolabelled for zn-1 (Fig. 2c).
13
14

15
16 There were no evident changes in the distribution pattern of zn1 until 4dpf when the
17
18 retina showed a great reduction of zn-1 immunoreactivity and zn-1-ir cells were only observed
19
20 in the outer most scleral part of the retina. Cells in the scleral part of the INL were segregated
21
22 into two groups. One was characterised by an elongated morphology and an arrangement
23
24 parallel to the OPL (Fig. 2d). The other was constituted by zn-1-ir cells with a thick stained
25
26 process directed towards the OPL, or reaching the nuclear layer of the retina (ONL) (Fig. 2e).
27
28 Because of their morphology and localisation we identified these cells as horizontal cells. At
29
30 this stage of development, there was no immunoreactivity for zn-1 in the axons of the ganglion
31
32 cells that constitute the optic nerve. At 4 dpf, zn-1-ir elements were observed in both the
33
34 dorsal-most part of the superficial white zone (SWZ) and in the PVGZ of the OT. The ventral-
35
36 most part of the SWZ did not present immunolabelled elements for zn-1 (Fig. 2f). From 4 dpf
37
38 onwards there was no immunoreactivity for zn-1 either in the visual pathway or in other
39
40 regions of the zebrafish CNS.
41
42
43
44
45
46
47
48
49

50 *3.2 Calretinin*

51
52 At 48 hpf, CR immunoreactive (CR-ir) elements in the anlage of the retinal INL were
53
54 observed. The stained prolongations of these cells arborised into the presumptive IPL
55
56 originating a scarce immunolabelled neuropile. These cells were identified as amacrine cells.
57
58 Some CR-ir ganglion cells were observed in the central part of the GCL. However, the axons
59
60
61
62
63
64
65

1
2
3 of the ganglion cells that constitute the optic nerve did not show immunoreactivity for CR at 48
4 hpf (Fig. 3a). Regarding the OT, CR-ir cells were observed only in the lateral portions. These
5
6 cells were situated in both the SWZ and the PVGZ, displaying a rounded morphology and
7
8 immunolabelled processes (Fig. 3a).
9
10

11
12
13 The CR distribution pattern in the retina at the 60 hpf stage was very similar to that
14
15 observed at the previous stage. The OT showed CR-ir cells and neuropile in both the lateral
16
17 and medial portions of the two germinal zones of the OT: SWZ and PVGZ (Fig. 3b).
18
19

20
21 After hatching, the density of CR-ir elements in the retina and OT increased. The CR
22
23 distribution pattern in the retina extended from the central part to its whole extension. In
24
25 addition, immunoreactivity for CR was detected in the optic nerve fibre layer of the retina
26
27 (ONFL) (Fig. 3c). Immunolabelled axons were observed in the optic nerve, optic chiasm and
28
29 optic tracts, and remained immunostained until adult life.
30
31

32
33 In the OT, the thickness of the SWZ was greater than previous stages and two regions
34
35 were discerned. The superficial most region had fusiform CR-ir cells and fibres. The deepest
36
37 region, in contact with the PVGZ, showed only CR-ir fibres and the density of CR-ir cells in
38
39 the PVGZ increased with respect to previous stages. At 3dpf CR-immunoreactivity was also
40
41 observed in the retino-ectal projections that arrived at the rostral most part of the OT (Fig. 3c).
42
43
44

45
46 At 4 dpf, in addition to the ganglion cells, immunoreactivity for CR in another cell type
47
48 in the GCL, with a pear-shaped morphology and single stained process directed towards the
49
50 IPL was observed. Due to morphology and localisation, these cells were identified as displaced
51
52 amacrine cells (Fig. 3d).
53

54
55 At 30 dpf the distribution of CR immunoreactivity in the retina was similar to that
56
57 observed at previous stages and in adult animals. Axons of the retino-pretectal-hypothalamic
58
59 and retino-hypothalamic pathways showed immunoreactivity for CR (Fig. 3e). From 3dpf to 30
60
61
62
63
64
65

1
2
3 dpf a refinement of the CR distribution was observed in the OT until all the layers were
4 developed. The OT displayed all the strata that will constitute the adult OT at this stage. From
5 the pial surface inwards the first tectal stratum was the marginal stratum (MS), which showed
6 CR-ir cells for the first time at this stage. The CR-ir cells had rounded morphology with one
7 immunolabelled prolongation. The optic stratum (OS) showed CR-ir fibres that correspond
8 with the axons of the ganglion cells. The superficial fibrous and grey stratum (SFGS) displayed
9 both CR-ir fibres and CR-ir rounded and fusiform cells. The central grey stratum (CGS) and
10 the central white stratum (CWS) showed a lower density of CR-ir cells compared with the
11 deepest stratum, the periventricular stratum (PVS). In the PVS, CR-ir cells showed a single
12 immunolabelled prolongation directed towards the more superficial tectal strata, arriving in
13 some cases at the SFGS (Fig. 3f). Using previous morphological criteria by Golgi impregnation
14 (Meek and Schellart, 1978), we identified these cells as type XIV neurons. There were no
15 significant changes in the CR distribution pattern between 30 dpf and 60 dpf.
16
17

18
19
20
21
22
23
24
25
26
27
28
29
30
31
32
33
34
35
36
37
38
39
40
41
42
43
44
45
46
47
48
49
50
51
52
53
54
55
56
57
58
59
60
61
62
63
64
65

In the retina of adult animals (90 dpf and 1 year), the CR-ir elements were ganglion cells and displaced amacrine cells in the GCL, amacrine cells in the INL and immunolabelled neuropile in the IPL (Fig. 3g). The retinofugal (retino-tectal, retino-prepecto-hypothalamic and retino-hypothalamic) projections remained CR immunoreactive, as observed in previous stages. Finally, the main change in the CR distribution pattern in the adult OT was the decrease in the density of CR-ir cells in the MS, which displayed a single stained process directed towards the OS (Fig. 3h).

3.3 Glial fibrillary acidic protein

At 36 hpf, GFAP-ir cell bodies and processes delimiting the lateral regions of the mesencephalic OT were observed (Fig. 4a). The intensity of the staining was stronger in the

1
2
3 ventral region (presumptive PVGZ) than in the dorsal region (presumptive SWZ). The
4
5 boundary between the caudal portion of the OT and the rhombencephalon also showed
6
7 immunoreactivity for GFAP.
8
9

10
11 At the end of embryonic life (60 hpf), zebrafish optic nerve showed immunoreactivity for
12
13 GFAP in both cell bodies and processes. The ventrolateral optic tract also displayed
14
15 immunoreactivity for GFAP (Fig. 4b). The rostral part of the OT was delimited by GFAP-ir
16
17 processes.
18
19

20
21 After hatching, GFAP-ir elements were observed in the retina close to the vitreal region.
22
23 GFAP-ir was also present in both cell bodies and processes of the optic nerve (Fig. 4c).
24
25

26
27 At the 5 dpf stage, the ONFL of the retina showed an increase in the density of GFAP-ir
28
29 processes with respect to previous stages (Fig. 4d). The immunoreactivity for GFAP was
30
31 identified as the endfeet of Müller cells. This staining was also observed in adult animals. No
32
33 immunolabelled processes were observed in the optic nerve.
34

35
36 At 30 dpf, GFAP-ir processes in all tectal bands were observed (Fig. 4e). The density of
37
38 GFAP-ir processes was higher in the rostral most portion of the OT than in the caudal most
39
40 region. There were no significant differences in the GFAP distribution pattern between 60 hpf
41
42 and 30 dpf. In adult animals GFAP-immunolabelled processes were observed in both the limit
43
44 of the OS and in the SFGS of the OT, close to the radial stained prolongations of the subpial
45
46 limitant (Fig. 4f).
47
48
49
50
51

52 *3.4 Double immunostaining*

53

54
55 At 3 dpf, the optic nerve of zebrafish larvae displayed immunoreactivity for both CR and
56
57 GFAP. The staining for CR was observed only in axons (Fig. 5a), while immunoreactivity for
58
59
60
61
62
63
64
65

1
2
3 GFAP was located in glial processes (Fig. 5b). Co-localisation of the immunostaining for CR
4
5 and GFAP was not observed (Fig. 5c).
6
7
8
9

10 11 12 13 **4. Discussion**

14
15 In this study we have analysed the distribution pattern of three molecular markers (zn-1,
16 CR, GFAP) during the morphogenesis of the zebrafish visual system. The immunodetection of
17 these proteins allows the study of the evolution of the cell populations and projections into
18 their adult configuration and the environment in which they develop.
19
20
21
22
23
24

25 In both zebrafish retina and OT, zn1 is expressed very early during embryonic
26 development (36 hpf), suggesting a putative role in morphofunctional differentiation of the
27 visual system. In the retina, CR and GFAP onsets are observed at the same stage of
28 development (48 hpf), while the OT displays an earlier expression of GFAP (36 pf) than CR
29 (48 hpf). Moreover, a transient expression of GFAP in cell bodies and processes in the optic
30 nerve is observed around hatching.
31
32
33
34
35
36
37
38
39
40
41

42 *4.1 Zn-1 in the fish visual pathway*

43
44 The studies using zn-1 are restricted to the rhombencephalon and myelencephalon of
45 zebrafish during embryonic development (Hanneman *et al.*, 1988; Trevarrow *et al.*, 1990) and
46 the auditive pathway of juvenile and adult zebrafish (Bang *et al.*, 2001). Regarding zn-1
47 functional implications, it has been suggested that zn-1 may be involved in the latter stages of
48 differentiation of the statoacoustic and auditive system in the axolotl *Ambystoma mexicanum*
49 (Kornblum *et al.*, 1990). The zn-1 immunoreactivity in zebrafish retina (present results) is
50
51
52
53
54
55
56
57
58
59
60
61
62
63
64
65

1
2
3 observed in the primordia of the GCL at the 36 hpf stage, when the first ganglion cell axons
4 exit the optic vesicle (Stuermer, 1988).
5
6
7
8
9

10 4.2 Calretinin in the fish visual pathway

11
12 During vertebrate development, CR is expressed in different cellular types and neuropile
13 and the onset of the immunoreactivity for CR coincides with the differentiation of the retinal
14 histological layers (Doldan *et al.*, 1999; present results).
15
16
17
18
19

20 The distribution pattern of the immunoreactivity for CR in the retina has been previously
21 analysed in three groups of teleostean fish with different habitats: cyprinidae (tench *Tinca*
22 *tinca*: Weruaga *et al.*, 2000; zebrafish: García-Crespo and Vecino, 2004; Castro *et al.*, 2006),
23 scophthalmidae (turbot *Psetta maxima*: Doldan *et al.*, 1999), salmonidae (rainbow trout
24 *Oncorhynchus mykiss*: Weruaga *et al.*, 2000) and petromyzontidae (lamprey: Villar-Cheda *et*
25 *al.*, 2006). The CR expression pattern is similar among the teleostean species studied since it
26 localises in neurons of the GCL and INL, where ganglion and amacrine cells are
27 immunolabelled for CR. However, there are some differences between species in the retinal
28 cellular types immunolabelled for CR. Previous works detected bipolar cells in different
29 teleosts (rainbow trout, Weruaga *et al.*, 2000; turbot, Doldan *et al.*, 1999; lamprey, Villar-
30 Cheda *et al.*, 2006) and also in the INL of zebrafish (Yazulla and Studholme, 2001). We have
31 not seen descending and ascending projections in the positive cells in the INL, thus we identify
32 them as amacrine cell. Double immunohistochemistry with specific antibodies of amacrine and
33 bipolar cells should be performed in order to answer this question. We have not detected
34 horizontal cells, which have been described in the turbot (Doldan *et al.*, 1999) and in the
35 lamprey (Villar-Cheda *et al.*, 2006).
36
37
38
39
40
41
42
43
44
45
46
47
48
49
50
51
52
53
54
55
56
57
58
59
60
61
62
63
64
65

1
2
3
4 During the development of the vertebrate retina, it has been suggested that a minimal
5
6 degree of cell and tissue differentiation is required for the CR expression (Ellis *et al.*, 1991;
7
8 Doldan *et al.*, 1999). The appearance of CR in the retina occurs concurrently with the
9
10 establishment of the early laminar organisation when the proliferation capability of neuroblast
11
12 is reduced (Mack and Fernald, 1997) and retinal cells acquire their neurochemical identity
13
14 (Negishi and Wagner, 1995). At this stage in ontogeny, CR could participate in the formation
15
16 of the firing pattern of neurons (Miller and Baimbridge, 1983), as well as triggering some
17
18 enzymes in the signal transduction machinery of cells (Yamaguchi *et al.*, 1991).
19
20
21

22
23 CR expression in adult OT has been analyzed in tench (Arévalo *et al.*, 1995) and
24
25 zebrafish (Castro *et al.*, 2006). Staining is very similar between these species but divergences
26
27 are described in the MS, with CR-ir cells in zebrafish (Castro *et al.*, 2006; present results), but
28
29 not in the tench (Arévalo *et al.*, 1995). The existence of CR-ir cells in the MS during juvenile
30
31 development (present results) could be a consequence of the continuous neurogenesis and
32
33 migration processes that this encephalic region presents in fish (review in Zupanc, 2008; Ito *et*
34
35 *al.*, 2010). The Cajal-Retzius cells in the marginal zone (prospective layer I) of the mammalian
36
37 cortex show CR-immunoreactivity during cortinogenesis (Weisenhorn *et al.*, 1994). It has been
38
39 suggested that these cells engaged in migration may need CR during this migratory period. The
40
41 CR-ir neurons in the MS of the fish OT could be considered a homologous cellular type of the
42
43 CR-ir Cajal-Retzius cells.
44
45
46
47
48
49
50
51

52 4.3 Glial fibrillary acidic protein in the fish visual pathway

53

54
55 The GFAP distribution pattern described in our studies is similar to that described in
56
57 other teleostean species (goldfish *Carassius auratus*: Nona *et al.*, 1989; carp *Cyprinus carpio*:
58
59 Kalmán, 1998; tench: Jimeno *et al.*, 1999; zebrafish: Bernardos and Raymond, 2006; Yazulla
60
61
62
63
64
65

1
2
3 and Studholme, 2001). GFAP-ir cells in the retina have been considered as astrocytic cells
4
5 although some authors have observed some oligodendroglial characteristics since these cells
6
7 can be identified using specific markers of both astrocytes and oligodendrocytes (Kumpulainen
8
9 *et al.*, 1983; Norenberg and Martínez-Hernández, 1979).

10
11
12
13 The optic nerve of zebrafish shows a transient expression of GFAP in glial cells around
14
15 hatching. In the teleostean optic nerve, only one type of astrocyte is considered, which is
16
17 denominated reticular (Maggs and Scholes, 1990), morphologically characterised by its regular
18
19 distribution along the nerve and the organisation of their prolongations that participate in the
20
21 nerve bundling. The GFAP, as a member of the cytoskeletal protein family, is thought to be an
22
23 important modulator of astrocyte motility and shape by providing structural stability to
24
25 astrocytic processes (Eng *et al.*, 2000).

26
27
28
29
30 The transient expression of GFAP in the optic nerve coincides with the arrival of the
31
32 majority of the zn-1-ir and CR-ir optic axons. Thus, glial cells could support early axon
33
34 outgrowth as it occurs in the zebrafish hindbrain (Marcus and Easter, 1995) and forebrain
35
36 commissures (Barresi *et al.*, 2005) and could be involved in the axonal guidance as it happens in
37
38 the chicken optic nerve (Gerhardt *et al.*, 2000).

39
40
41
42 The retinorecipient tectal strata and the retina are the two main regions that support axon
43
44 guidance in the zebrafish visual pathway and they show GFAP immunoreactiviy during
45
46 ontogeny. Radial glia could be involved in the migration of neuroblasts from the PVS to the
47
48 rest of the tectal strata (Schmatolla and Erdmann, 1973; Ito *et al.*, 2010), as well as in other
49
50 regions of the fish CNS (Bauchot *et al.*, 1979; Tomizawa *et al.*, 2000).

51 52 53 54 55 56 57 **Acknowledgments** 58 59 60 61 62 63 64 65

1
2
3
4 This work was supported by funds from the MICINN (BFU2009-11179) and Junta de
5
6 Castilla yLeón (Grupo de Excelencia GR-183 and Consejería de Sanidad). The authors would
7
8 like to thank Miss M.T. Sánchez and Dr. J. Herrero-Turrión for her technical assistance, and
9
10 Mr. G. H. Jenkins for his help with the English version of the manuscript.
11
12
13
14
15
16
17
18
19
20
21
22
23
24
25
26
27
28
29
30
31
32
33
34
35
36
37
38
39
40
41
42
43
44
45
46
47
48
49
50
51
52
53
54
55
56
57
58
59
60
61
62
63
64
65

References

- Amsterdam, A., Hopkins, N., 2006. Mutagenesis strategies in zebrafish for identifying genes involved in development and disease. *Trends Genet.* 22(9), 473-478.
- Arenzana, F.J., Clemente, D., Sánchez-González, R., Porteros, A., Aijón, J., Arévalo, R., 2005. Development of the cholinergic system in the brain and retina of the zebrafish. *Brain. Res. Bull.* 66, 421-425.
- Arenzana, F.J., Arévalo, R., Sánchez-González, R., Clemente, D., Aijón, J., Porteros, A., 2006. Tyrosine hydroxylase immunoreactivity in the developing visual pathway of the zebrafish. *Anat. Embryol.* 211(4), 323-334.
- Arévalo, R., Alonso, J.R., Porteros, A., Briñón, J.G., Crespo, C., Lara, J., Aijón, J., 1995. Calretinin-like immunoreactivity in the optic tectum of the tench (*Tinca tinca* L.). *Brain Res.* 671, 112-118.
- Bang, P.I., Sewell, W.F., Malicki, J.J., 2001. Morphology and cell type heterogeneities of the inner ear epithelia in adult and juvenile zebrafish (*Danio rerio*). *J. Comp. Neurol.* 438, 173-190.
- Barresi, M.J., Hutson, L.D., Chien, C.B., Karlstrom, R.O., 2005. Hedgehog regulated Slit expression determines commissure and glial cell position in the zebrafish forebrain. *Development* 132(16), 3643-3656.
- Bauchot, R., Diagne, M., Ribet, J.M., 1979. Post-hatching growth and allometry of the teleost brain. *J. Hirnforsch.* 20, 29-34.
- Bernardos, R.L., Raymond, P.A., 2006. GFAP transgenic zebrafish. *Gene Expr. Patterns* 6, 1007-1013.

- 1
2
3 Burrill, J.D., Easter, S.S. Jr., 1994. Development of the retinofugal projections in the
4 embryonic and larval zebrafish (*Brachydanio rerio*). *J. Comp. Neurol.* 346(4), 583-600.
5
6
7
8 Candal, E., Ferreiro-Galve, S., Anadón, R., Rodríguez-Moldes, I., 2008. Morphogenesis in the
9 retina of a slow-developing teleost: emergence of the GABAergic system in relation to
10 cell proliferation and differentiation. *Brain Res.* 1194, 21-27.
11
12
13
14
15 Cardone, B., Roots, B.I., 1990. Comparative immunohistochemical study of glial filament
16 proteins (glial fibrillary acidic protein and vimentin) in goldfish, octopus, and snail. *Glia*
17 3, 180-192.
18
19
20
21
22
23 Castro, A., Becerra, M., Manso, M.J., Anadón, R., 2006. Calretinin immunoreactivity in the
24 brain of the zebrafish, *Danio rerio*: distribution and comparison with some neuropeptides
25 and neurotransmitter-synthesizing enzymes. II. Midbrain, hindbrain, and rostral spinal
26 cord. *J. Comp. Neurol.* 494, 792–814.
27
28
29
30
31
32
33 Cerveny, K.L., Cavodeassi, F., Turner, K.J., de Jong-Curtain, T.A., Heath, J.K., Wilson, S.W.,
34 2010. The zebrafish flotte lotte mutant reveals that the local retinal environment promotes
35 the differentiation of proliferating precursors emerging from their stem cell niche.
36 *Development* 137(13), 2107-2115.
37
38
39
40
41
42
43 Clemente, D., Porteros, A., Weruaga, E., Alonso, J.R., Arenzana, F.J., Aijón, J., Arévalo, R.,
44 2004. Cholinergic elements in the zebrafish central nervous system: Histochemical and
45 immunohistochemical analysis. *J. Comp. Neurol.* 474(1), 75-107.
46
47
48
49
50 Clemente D., Porteros A., Arenzana F.J., Aijón J., Parrilla M., Santos-Ledo A., Arévalo R.,
51 2008. Characterization of NADPH-diaphorase-positive glial cells of the tench optic nerve
52 after axotomy. *Arch. Ital. Biol.* 146(1), 35-52.
53
54
55
56
57 Davis R.E., Northcutt R.G., 1983. Evolution of the optic tectum in ray-finned fishes (*Fish*
58 *Neurobiology*, Vol2), 1-42.
59
60
61
62
63
64
65

- 1
2
3
4 Díaz M.L., Becerra M., Manso M.J., Anadón R., 2002. Distribution of thyrotropin-releasing
5
6 hormone (TRH) immunoreactivity in the brain of the zebrafish (*Danio rerio*). J Comp
7
8 Neurol. 450(1), 45-60.
9
- 10
11 Doldan, M.J., Prego, B., de Miguel, V., 1999. Immunochemical localization of calretinin in the
12
13 retina of the turbot (*Psetta maxima*) during development. J. Comp. Neurol. 406, 425-432.
14
- 15
16 Easter, S.S., Nicola, G.N., 1996. The development of vision in the zebrafish (*Danio rerio*).
17
18 Dev. Biol. 180, 646-663.
19
- 20
21 Ellis, J.H., Richards, D.E., Rogers, J.H., 1991. Calretinin and calbindin in the retina of the
22
23 developing chick. Cell Tissue Res. 264, 197-208.
24
- 25
26 Emran, F., Rihel, J., Adolph, A.R., Dowling, J.E., 2010. Zebrafish larvae lose vision at night.
27
28 Proc. Natl. Acad. Sci. U. S. A. 107(13), 6034-6039.
29
- 30
31 Eng, L.F., Ghirnikar, R.S., Lee, Y.L., 2000. Glial fibrillary acidic protein: GFAP-thirty-one
32
33 years (1969-2000). Neurochem. Res. 25, 1439-1451.
34
- 35
36 Fadool, J.M., Dowling, J.E., 2008. Zebrafish: a model system for the study of eye genetics.
37
38 Prog. Retin. Eye Res. 27(1), 89-110.
39
- 40
41 Faraco, J.H., Appelbaum, L., Marin, W., Gaus, S.E., Mourrain, P., Mignot, E., 2006.
42
43 Regulation of hypocretin (orexin) expression in embryonic zebrafish. J. Biol. Chem.
44
45 281(40), 29753-29761.
46
- 47
48 Filippi, A., Dürr, K., Ryu, S., Willaredt, M., Holzschuh, J., Driever, W., 2007. Expression and
49
50 function of *nr4a2*, *lmx1b*, and *pitx3* in zebrafish dopaminergic and noradrenergic
51
52 neuronal development. BMC Dev. Biol. 7, 135.
53
- 54
55 Filippi, A., Mahler, J., Schweitzer, J., Driever, W., 2010. The subtype-selective nicotinic
56
57 acetylcholine receptor positive allosteric potentiator 2087101 differentially facilitates
58
59 neurotransmission in the brain. Eur. J. Pharmacol. 643(2-3), 218-224.
60
61
62
63
64
65

- 1
2
3
4
5
6
7
8
9
10
11
12
13
14
15
16
17
18
19
20
21
22
23
24
25
26
27
28
29
30
31
32
33
34
35
36
37
38
39
40
41
42
43
44
45
46
47
48
49
50
51
52
53
54
55
56
57
58
59
60
61
62
63
64
65
- García-Crespo, D., Vecino, E., 2004. Differential expression of calretinin in the developing and regenerating zebrafish visual system. *Histol. Histopathol.* 19, 1193-1199.
- Gerhardt, H., Rascher, G., Schuck, J., Weigold, U., Redies, C., Wolburg, H., 2000. R- and B-cadherin expression defines subpopulations of glial cells involved in axonal guidance in the optic nerve head of the chicken. *Glia* 31(2), 131-143.
- Goldsmith, P., Harris, W.A., 2003. The zebrafish as a tool for understanding the biology of visual disorders. *Semin. Cell Dev. Biol.* 14(1), 11-18.
- Hanneman, E., Trevarrow, B., Metcalfe, W.K., Kimmel, C.B., Westerfield, M., 1988. Segmental pattern of development of the hindbrain and spinal cord of the zebrafish embryo. *Development* 103, 49-58.
- Henshall, T.L., Tucker, B., Lumsden, A.L., Nornes, S., Lardelli, M.T., Richards, R.I., 2009. Selective neuronal requirement for huntingtin in the developing zebrafish. *Hum. Mol. Genet.* 18(24), 4830-4842.
- Holmqvist, B., Ellingsen, B., Forsell, J., Zhdanova, I., Alm, P., 2004. The early ontogeny of neuronal nitric oxide synthase systems in the zebrafish. *J. Exp. Biol.* 207(6), 923-935.
- Holzschuh, J., Ryu, S., Aberger, F., Driever, W., 2001. Dopamine transporter expression distinguishes dopaminergic neurons from other catecholaminergic neurons in the developing zebrafish embryo. *Mech. Dev.* 101(1-2), 237-243.
- Ito, Y., Tanaka, H., Okamoto, H., Ohshima, T., 2010. Characterization of neural stem cells and their progeny in the adult zebrafish optic tectum. *Dev. Biol.* 342(1), 26-38.
- Jimeno, D., Velasco, A., Lillo, C., Lara, J.M., Aijón, J., 1999. Response of microglial cells after a cryolesion in the peripheral proliferative retina of tench. *Brain Res.* 816, 175-189.

- 1
2
3 Kalmán, M., 1998. Astroglial architecture of the carp (*Cyprinus carpio*) brain as revealed by
4 immunohistochemical staining against glial fibrillary acidic protein (GFAP). *Anat.*
5
6
7
8
9
10
11 Karlstrom, R.O., Trowe, T., Klostermann, S., Baier, H., Brand, M., Crawford, A.D.,
12
13
14
15
16
17
18
19
20
21
22
23
24
25
26
27
28
29
30
31
32
33
34
35
36
37
38
39
40
41
42
43
44
45
46
47
48
49
50
51
52
53
54
55
56
57
58
59
60
61
62
63
64
65
- Kalmán, M., 1998. Astroglial architecture of the carp (*Cyprinus carpio*) brain as revealed by immunohistochemical staining against glial fibrillary acidic protein (GFAP). *Anat. Embryol.* 198, 409-433.
- Karlstrom, R.O., Trowe, T., Klostermann, S., Baier, H., Brand, M., Crawford, A.D., Grunewald, B., Haffter, P., Hoffmann, H., Meyer, S.U., Müller, B.K., Richter, S., van Eeden, F.J., Nüsslein-Volhard, C., Bonhoeffer, F., 1996. Zebrafish mutations affecting retinotectal axon pathfinding. *Development* 123, 427-438.
- Kaslin, J., Panula, P., 2001. Comparative anatomy of the histaminergic and other aminergic systems in zebrafish (*Danio rerio*). *Comp. Neurol.* 440(4), 342-77.
- Kastenhuber, E., Kratochwil, C.F., Ryu, S., Schweitzer, J., Driever, W., 2010. Genetic dissection of dopaminergic and noradrenergic contributions to catecholaminergic tracts in early larval zebrafish. *J Comp Neurol.* 518(4), 439-458.
- Kornblum, H.I., Corwin, J.T., Trevarrow, B., 1990. Selective labeling of sensory hair cells and neurons in auditory, vestibular, and lateral line systems by a monoclonal antibody. *J. Comp. Neurol.* 301, 162-170.
- Kumpulainen, T., Dahl, D., Korhonen, L.K., Nystrom, S.H., 1983. Immunolabeling of carbonic anhydrase isoenzyme C and glial fibrillary acidic protein in paraffin-embedded tissue sections of human brain and retina. *J. Histochem. Cytochem.* 31, 879-886.
- Li, L., Li, Y., Chen, D., Shao, J., Li, X., Xu, C., 2010. Fishing for age-related visual system mutants: behavioral screening of retinal degeneration genes in zebrafish. *Curr. Aging Sci.* 3(1), 43-45.
- Lieschke, G.J., Currie, P.D., 2007. Animals models of human disease: zebrafish swim into view. *Nat. Rev. Genet.* 8(5), 353-367.

- 1
2
3
4 Liu, Q., Sanborn, K.L., Cobb, N., Raymond, P.A., Marrs, J.A., 1999. R-cadherin expression in
5
6 the developing and adult zebrafish visual system. *J. Comp. Neurol.* 410(2), 303-319.
7
8 Mack, A.F., Fernald, R.D., 1997. Cell movement and cell cycle dynamics in the retina of the
9
10 adult teleost *Haplochromis burtoni*. *J. Comp. Neurol.* 388, 435-443.
11
12 Maggs, A., Scholes, J., 1990. Reticular astrocytes in the fish optic nerve: macroglia with
13
14 epithelial characteristics form an axially repeated lacework pattern, to which nodes of
15
16 ranvier are apposed. *J. Neurosci.* 16, 1600-1614.
17
18
19
20 Marcus, R.C., Easter S.S. Jr., 1995. Expression of glial fibrillary acidic protein and its
21
22 relation to tract formation in embryonic zebrafish (*Danio rerio*). *J. Comp. Neurol.*
23
24 359(3), 365-381.
25
26
27
28 McLean, D.L., Fetcho, J.R., 2004. Ontogeny and innervation patterns of dopaminergic,
29
30 noradrenergic, and serotonergic neurons in larval zebrafish. *J. Comp. Neurol.* 480(1), 38-
31
32 56.
33
34
35 Meek, J., Nieuwenhuys, R., 1998. Holosteans and teleosts. In: *The Central Nervous System*
36
37 of Vertebrates, vol 2 (eds Nieuwenhuys, R., Ten Donkelaar, H.J., Nicholson, C.), 759-
38
39 938. Springer, Berlin
40
41
42 Meek, J., Schellart, N.A., 1978. A Golgi study of goldfish optic tectum. *J. Comp. Neurol.*
43
44 182(1), 89-122.
45
46
47 Miguel-Hidalgo J.J., Ito H. and Lara J., 1991. Distribution of calbindin-like immunoreactive
48
49 structures in the optic tectum of normal and eye-enucleated cyprinid fish. *Cell Tissue*
50
51 *Res.* 265, 511-516.
52
53
54
55 Miller, J.J., Baimbridge, K.G., 1983. Biochemical and immunohistochemical correlates of
56
57 kindling-induced epilepsy: role of calcium binding protein. *Brain Res.* 278, 322-326.
58
59
60
61
62
63
64
65

- 1
2
3
4 Mueller, T., Guo, S., 2009. The distribution of GAD67-mRNA in the adult zebrafish (teleost)
5
6 forebrain reveals a prosomeric pattern and suggests previously unidentified homologies
7
8 to tetrapods. *J. Comp. Neurol.* 516(6), 553-568.
9
- 10
11 Negishi, K., Wagner, H.J., 1995. Differentiation of photoreceptors, glia, and neurons in the
12
13 retina of the cichlid fish *Aequidens pulcher*; an immunocytochemical study. *Brain Res.*
14
15 *Dev. Brain Res.* 89, 87-102.
16
17
- 18
19 Newman, M., Tucker, B., Nornes, S., Ward, A., Lardelli, M., 2009. Altering presenilin gene
20
21 activity in zebrafish embryos causes changes in expression of genes with potential
22
23 involvement in Alzheimer's disease pathogenesis. *J. Alzheimers Dis.* 16(1), 133-147.
24
- 25
26 Nona, S.N., Shehab, S.A.S., Stafford, C.A., Cronly-Dillon, J.R., 1989. Glial fibrillary acidic
27
28 protein (GFAP) in goldfish. Its localisation in visual pathway. *Glia* 2, 189-200.
29
- 30
31 Norenberg, M.D., Martínez-Hernandez, A., 1979. Fine structural localization of glutamine
32
33 synthetase in astrocytes of rat brain. *Brain Res.* 161, 303-310.
34
- 35
36 Paquet, D., Bhat, R., Sydow, A., Mandelkow, E.M., Berg, S., Hellberg, S., Fälting, J., Distel,
37
38 M., Köster, R.W., Schmid, B., Haass, C., 2009. A zebrafish model of tauopathy allows in
39
40 vivo imaging of neuronal cell death and drug evaluation. *J. Clin. Invest.* 119(5), 1382-
41
42 1395.
43
- 44
45 Parng, C., Roy, N.M., Ton, C., Lin, Y., McGrath, P., 2007. Neurotoxicity assessment using
46
47 zebrafish. *J. Pharmacol. Toxicol. Methods* 55(1), 103-112.
48
49
- 50
51 Porteros, A., Arévalo, R., Weruaga, E., Crespo, C., Briñón, J.G., Alonso, J.R., Aijón, J., 1997.
52
53 Calretinin immunoreactivity in the developing olfactory system of the rainbow trout.
54
55 *Brain Res. Dev. Brain Res.* 100, 101-109.
56
57
58
59
60
61
62
63
64
65

- 1
2
3
4 Porteros, A., Briñón, J.G., Arévalo, R., Crespo, C., Aijón, J., Alonso, J.R., 1998. Transient
5
6 expression of calretinin in the trout habenulo-interpeduncular system during
7
8 development. *Neurosci. Lett.* 254, 9-12.
9
- 10 Prober, D.A., Rihel, J., Onah, A.A., Sung, R.J., Schier, A.F., 2006. Hypocretin/orexin
11
12 overexpression induces an insomnia-like phenotype in zebrafish. *J. Neurosci.* 26(51),
13
14 13400-13410.
15
16
- 17 Renninger, S.L., Schonthaler, H.B., Neuhauss, S.C., Dahm, R., Investigating the genetics of
18
19 visual processing, function and behaviour in zebrafish. *Neurogenetics.*
20
21
22
23
- 24 Sager, J.J., Bai, Q., Burton, E.A., 2010. Transgenic zebrafish models of neurodegenerative
25
26 diseases. *Brain Struct. Funct.* 214(2-3), 285-302.
27
28
- 29 Schmatolla, E., Erdmann, G., 1973. Influence of retino-tectal innervation on cell proliferation
30
31 and cell migration in the embryonic teleost tectum. *J. Embryol. Exp. Morphol.* 29, 697-
32
33 712.
34
35
- 36 Schmitt, E.A., Dowling, J.E., 1994. Early eye morphogenesis in the zebrafish, *Brachydanio*
37
38 *rerio*. *J. Comp. Neurol.* 344, 532-542.
39
40
- 41 Sharma, S.C. 1975. Development of the optic tectum in brown trout, in: Ali, M.A. (Eds.),
42
43 Vision in fishes. New approach in research. Plenum Press, New York, pp. 411-417.
44
45
- 46 Sheng, D., Qu, D., Kwok, K.H., Ng, S.S., Lim, A.Y., Aw, S.S., Lee, C.W., Sung, W.K., Tan,
47
48 E.K., Lufkin, T., Jesuthasan, S., Sinnakaruppan, M., Liu, J., 2010. Deletion of the WD40
49
50 domain of LRRK2 in Zebrafish causes Parkinsonism-like loss of neurons and locomotive
51
52 defect. *PLoS Genet.* 6(4), e1000914.
53
54
55
- 56 Sprague, J., Bayraktaroglu, L., Bradford, Y., Conlin, T., Dunn, N., Fashena, D., Frazer, K.,
57
58 Haendel, M., Howe, D.G., Knight, J., Mani, P., Moxon, S.A., Pich, C., Ramachandran,
59
60
61
62
63
64
65

1
2
3 S., Schaper, K., Segerdell, E., Shao, X., Singer, A., Song, P., Sprunger, B., Van Slyke,
4
5 C.E., Westerfield, M., 2008. The Zebrafish Information Network: the zebrafish model
6
7 organism database provides expanded support for genotypes and phenotypes. *Nucleic*
8
9 *Acids Res.* 36, D768-772.

10
11
12
13 Stuermer, C.A.O., 1988. Retinotopic organization of the developing retinotectal projection in
14
15 the zebrafish embryo. *J. Neurosci.* 8, 4513-4530.

16
17
18 Tomizawa, K., Inoue, Y., Nakayasu, H., 2000. A monoclonal antibody stains radial glia in the
19
20 adult zebrafish (*Danio rerio*) CNS. *J. Neurocytol.* 29(2), 119-128.

21
22
23 Trevarrow, B., Marks, D.L., Kimmel, C.B., 1990. Organization of hindbrain segments in the
24
25 zebrafish embryo. *Neuron.* 4, 669-679.

26
27
28 Trowe, T., Klostermann, S., Baier, H., Granato, M., Crawford, A.D., Grunewald, B.,
29
30 Hoffmann, H., Karlstrom, R.O., Meyer, S.U., Müller, B., Richter, S., Nüsslein-Volhard,
31
32 C., Bonhoeffer, F., 1996. Mutations disrupting the ordering and topographic mapping of
33
34 axons in the retinotectal projection of the zebrafish, *Danio rerio*. *Development* 123, 439-
35
36 450.

37
38
39 Vanegas, H., Ebbesson, S.O.E., Laufer, M., 1984. Morphological aspects of the teleostean
40
41 optic tectum. In *Comparative Neurology of the optic tectum* (ed Vanegas H), :93-120.
42
43 Plenum Pres, New York.

44
45
46
47 Villar-Cheda, B., Abalo, X.M., Anadón, R., Rodicio, M.C., 2006. Calbindin and calretinin
48
49 immunoreactivity in the retina of adult and larval sea lamprey. *Brain Res.* 1068(1), 118-
50
51 130.

52
53
54 Weisenhorn, D.M., Prieto, E.W., Celio, M.R., 1994. Localization of calretinin in cells of layer I
55
56 (Cajal-Retzius cells) of the developing cortex of the rat. *Brain Res. Dev. Brain Res.* 82,
57
58 293-297.
59
60
61
62
63
64
65

- 1
2
3 Weruaga, E., Velasco, A., Briñón, J.G., Arévalo, R., Aijón, J., Alonso, J.R., 2000. Distribution
4 of the calcium-binding proteins parvalbumin, calbindin D-28k and calretinin in the retina
5
6 of two teleosts. *J. Chem. Neuroanat.* 19, 1-15.
7
8
9
- 10
11 Westerfield, M., 1995. *The Zebrafish Book. A guide for the laboratory use of zebrafish (Danio*
12
13 *rerio)*. University of Oregon, Eugene, 363.
14
- 15
16 Wilson, S.W., Houart, C., 2004. Early steps in the development of the forebrain. *Dev Cell.*
17
18 6(2), 167-181.
19
- 20
21 Yamaguchi, T., Winsky, L., Jacobowitz, D.M., 1991. Calretinin, a neuronal calcium binding
22
23 protein, inhibits phosphorylation of a 39 kDa synaptic membrane protein from rat brain
24
25 cerebral cortex. *Neurosci. Lett.* 131, 79-82.
26
- 27
28 Zupanc G.K., 2008. Adult neurogenesis and neuronal regeneration in the brain of teleost fish.
29
30 *J. Physiol. Paris.* 102(4-6):357-73. Review.
31
32
33
34
35
36
37
38
39
40
41
42
43
44
45
46
47
48
49
50
51
52
53
54
55
56
57
58
59
60
61
62
63
64
65

1
2
3
4
5
6 **Figure legends**
7

8 **Fig. 1:** Western blots of zebrafish and mouse retina and brain extracts with the anti-
9 GFAP monoclonal antibody displaying a single band around 50 kDa in all lanes.
10
11
12
13
14

15 **Fig. 2:** (a) Parasagittal section of the rostralmost part of an embryo at 36 hpf showing zn-
16 1-ir elements in both the central part of the presumptive GCL (arrowhead) and the PVGZ
17 (arrow). (b) Parasagittal section of an embryo at 36 hpf showing zn-1-ir elements in the PVGZ
18 (arrows) of the OT. (c) Immunoreactivity for zn-1 in the ganglion cell axons constituting the
19 optic nerve (arrow) at 48 hpf. (d, e) Retina of larvae at 4 dpf showing two groups of zn-1-ir
20 cells. One of them is constituted by elongated adjacent zn-1-ir cells, in a parallel orientation
21 with respect to the retinal lamination (arrow in d). The other group is composed by cells in a
22 perpendicular orientation with a thick stained process directed towards the OPL or the ONL
23 (arrowheads in e). (f) OT of larva at 4 dpf showing zn-1 immunolabeling in the dorsal part of
24 the SWZ (arrow) and in the PVGZ (arrowheads in inset). Scale bar: c, d, e = 50 μ m; a, b, f,
25 inset in f = 100 μ m. D: diencephalon; dpf: days post-fertilization; GCL: ganglion cell layer; H:
26 hypothalamus; hpf: hours post-fertilization; M: mesencephalon; ONL: outer nuclear layer;
27 OPL: outer plexiform layer; OT: optic tectum; PVGZ: periventricular grey zone; T:
28 telencephalon.
29
30
31
32
33
34
35
36
37
38
39
40
41
42
43
44
45
46
47
48
49
50
51

52 **Fig. 3:** (a) Transversal section of an embryo at 48 hpf showing CR-ir cells in the
53 presumptive GCL (arrowhead) and in the presumptive INL. CR-ir cells are present in the
54 PVGZ of the OT (arrow). (b) Parasagittal section of the zebrafish encephalon at 60 hpf
55 showing CR-ir cells in the T, in the PVGZ and SWZ of the OT and in the ventral part of the H.
56
57
58
59
60
61
62
63
64
65

1
2
3 (c) CR-ir elements are present in the SWZ (arrow) and in the PVGZ of the OT.
4
5 Immunolabelled axons (arrowhead) can be observed in the optic nerve, optic chiasm and optic
6
7 tracts. (d) Section of a retina at 4 dpf stage, another cell type with a pear-shaped morphology
8
9 and single stained process directed towards the IPL is observed (arrow). (e) Parasagittal
10
11 section at 30 dpf that shows the immunostaining in the optic nerve (arrow) and in the retino-
12
13 pretectal-hypothalamic pathway (arrowhead). (f) CR distribution pattern in all the tectal bands
14
15 showing CR-ir neuropile in all tectal bands and stained cells in the MS (arrow) and the SFGS
16
17 (arrowhead). (g) In the retina of adult animals, CR-ir elements are ganglion cells and displaced
18
19 amacrine cells in the GCL, amacrine cells in the INL and immunolabelled neuropile in the IPL.
20
21 The optic nerve is positive for CR (arrowhead). (h) At 1 year, positive cells for CR are
22
23 observed in the MS (arrow) although in a reduced number. Scale bar: a, b, c, f, g= 100 μ m; e =
24
25 200 μ m. CGS: central grey stratum; CWS: central white stratum; dpf: days post-fertilization;
26
27 GCL: ganglion cell layer; hpf: hours post-fertilization; H: hindbrain; INL: inner nuclear layer;
28
29 IPL: inner plexiform layer; M: mesencephalon; MS: marginal stratum; ONL: outer nuclear
30
31 layer; OPL: outer plexiform layer; OS: optic stratum; OT: optic tectum; PE: pigmentary
32
33 epithelium; PVGZ: periventricular grey zone; PVS: periventricular stratum; SFGS: superficial
34
35 fibrous and grey stratum; SWZ: superficial white zone; T: telencephalon.
36
37
38
39
40
41
42
43
44
45
46

47 **Fig. 4:** (a) Parasagittal section of the zebrafish CNS at 36 hpf that shows the boundaries
48
49 of mesencephalic OT by GFAP-ir processes (arrow). (b) Transversal section at diencephalic
50
51 level at 60 hpf showing GFAP staining in both cell bodies and processes of optic tract in the
52
53 dorsomedial portion of this encephalic region (arrows). (c) GFAP-ir cell bodies and processes
54
55 in the optic nerve (arrow) at 3 dpf (magnification in enlarged area). (d) At 5 dpf, GFAP-ir
56
57 processes (arrow) of the retina are observed in the ONFL. (e) GFAP-ir distribution pattern in
58
59
60
61
62
63
64
65

1
2
3 the different strata of the OT at 30 dpf. All the tectal strata show GFAP stained processes with
4
5 the exception of the MS. (f) The staining for GFAP in zebrafish OT at 1 year is only observed
6
7 in the SFGS and in the OS. Scale bar: inset in c: 10 μm ; c, d: 50 μm ; a, b, e, f = 100 μm . CGS:
8
9 central grey stratum; CWS: central white stratum; dpf: days post-fertilization; hpf: hours post-
10
11 fertilization; M: mesencephalon; MS: marginal stratum; ONFL: optic nerve fibre layer; OS:
12
13 optic stratum; OT: optic tectum; PVS: periventricular stratum; R: rombencephalon; SFGS:
14
15 superficial fibrous and grey stratum.
16
17
18
19
20
21
22

23 **Fig. 5:** Horizontal sections of zebrafish brain at 3 dpf showing the optic nerve and double
24
25 immunohistochemical detection of calretinin (CR) and glial fibrillary acidic protein (GFAP).
26
27 (a) CR immunoreactivity in zebrafish optic nerve is observed only in neuropile (arrow). (b)
28
29 GFAP-ir processes in the optic nerve (asterisks). (c) The CR-ir optic axons (arrow) and GFAP-
30
31 ir glial processes (asterisks) are close but co-localization is not observed. The nuclei are
32
33 counterstained with propidium iodide (PI). Scale bar: a, b, c = 40 μm . INL: inner nuclear layer;
34
35
36
37
38 ONL: outer nuclear layer.
39
40
41
42
43
44
45
46
47
48
49
50
51
52
53
54
55
56
57
58
59
60
61
62
63
64
65

